RESEARCHERID
THOMSON REUTERS

[Reddy* *et al.*, 6(5): May, 2017]
IC™ Value: 3.00

ISSN: 2277-9655
Impact Factor: 4.116
CODEN: IJESS7

IJESRT

INTERNATIONAL JOURNAL OF ENGINEERING SCIENCES & RESEARCH TECHNOLOGY

RELIABILITY ANALYSIS OF ANOMALIES AND DISEASE PREDICTION USING NOVEL OPTIMAL SEGMENTATION FRAMEWORK FOR VARIOUS NON – EQUILIBRIUM BRAIN TISSUE ANGULAR MOMENTUM

Nageswara Reddy P*, C.P.V.N.J.Mohan Rao, Ch.Satyanarayana
* Research Scholar, Jawaharlal Nehru Technological University, Kakinada
Professor and Principal, Avanthi Institute of Engineering & Technology
Professor, Department of computer Science and Engineering, JNTU Kakinada

DOI: 10.5281/zenodo.573547

ABSTRACT

With the growing need for clinical diagnosis accuracy, the need for automation or computer aided analysis is also growing. Moderate numbers of methods are introduced to analyse the biological symptoms and produce the report to be recognized by the trained professions. Conversely, the final analysis is prone to errors due because of human interpretations. Also the computer aided reports leave huge scope for multiple further diagnoses. Thus the need of a novel algorithm for predictive analysis of diseases for brain disorder is much expected. This paper presents a fully reliable brain disease detection mechanism based on an enhancement in accuracy of multilateral filter and applied watershed method with EM-GM method. The proposed optimal unification method is timely and optimal methods to process the optimal sets of segments are divided and finest merged results. The multilateral filter enhances the image edges for better segmentation using signal amplitude moderation of the pixel. The final outcome of this paper produces the brain regions detected with anomalies and possible diseases, thus the number of possible further medical investigations are reduced.

KEYWORDS: Brain MR Images, T1, T2, T1C, Flair, HMA, Watershed Method, EM-GM Method, Multilateral Filter, Optimal Unification, Disorder Detection.

INTRODUCTION

The MRI or the Magnetic Resonance Image is a powerful method to capture the cranial structure and produce a computerized image for further analysis. The main reason of the popularity of this technique is non-ionizing radiation. To maximize the accuracy, this technique has extended the information inside the images. Thus the analysis of this complex and high quality images became the most tedious task for the technicians. Moreover, due to the human intervention the investigations are bound to be erroneous. Also these manual analyses are often time-consuming and limited in finding difficulties in brain data analysis compared to the computerized methods for anomalies detection [1].

The output format of MR technique depends on the signal of the magnetic field and how it deteriorates commonly known as relaxation. The relaxation is the pure reflection of the magnetic resonance. The analysis of relaxation denotes the speed of recovery for each cell or a region after population. The standard measures for each type of cells are predefined as per the medical standard, hence any abnormality observed is considered as anomaly. This work demonstrates the differentiating factors for each type of image outputs with the mathematical interpretations. Also, this work extends the analysis of proposed framework on various types of images.

The best possible analyses of image for detecting differences in regions are the segmentation techniques. Segmentation is applied to medical purposes like analysis of brain cell distortion, regions with damaged cells, anatomical visualization and planning for brain surgery by many researchers. Though limitations identified from the study demonstrate various segmentation techniques are restricted in generating high accuracy and mostly focused in brain tumor detection. The recent researches also fail to achieve the unsurpassed accuracy [2].

ISSN: 2277-9655
Impact Factor: 4.116
CODEN: IJESS7

Henceforth the rest of the paper is furnished with the focus to exhibit the improvement in accuracy of disorder detection for T1, T2, T1C and FLAIR type MR Images.

LONGITUDINAL RELAXATION TIME VARIATIONS

The fundamental basis of any MR imaging technique depends on the magnetization vector property. Based on spin – lattice or spin – spin relationship multiple MR images are been produced. In this section, the analyses of various image types are listed.

A. T1 Type Image

The Spin – Lattice relaxation time or T1 variant image is denoted as decay constant for the recovery time for the spin magnetization.

Denoted as,

$$M_z = M_{z,eq} - [M_{z,eq} - M_z(0)]\,e^{-t/T_1} \quad \text{(Eq. 1)}$$

Where,

$M_{z,eq}$ is the thermal equilibrium value for the MR

M_z is the spin magnetization value

Hence, the T1 can be defined as

$$e^{-t/T_1} = M_z / M_{z,eq} - [M_{z,eq} - M_z(0)] \quad \text{(Eq. 2)}$$

B. T2 Type Image

The transverse spin to spin relaxation time T2 is the decay constant for the recovery time for the spin magnetization, where the magnetization vector decays towards the equilibrium.

Denoted as,

$$M_{xy}(t) = M_{xy}(0)e^{-t/T_2} \quad \text{(Eq. 3)}$$

Where,

$M_{xy}(t)$ is the spin magnetization value

Hence, the T2 can be defined as

$$e^{-t/T_2} = M_{xy}(t) / M_{xy}(0) \quad \text{(Eq. 4)}$$

C. T1C Image

The T1C is the concentrated Spin – Lattice relaxation imaging which is similar to T1 images with the higher concentration of the magnetic resonance magnitudes. The details of the T1 image is already been showcased in the previous sub section.

D. FLAIR Image

The FLAIR or Fluid Attenuated Inversion Recovery is also a type of image generated by magnetic resonance to visualize the pulse sequence. The pulse sequence can be obtained by applying Fourier transform on any magnetic relaxation outputs and applying the decay. Hence, the outcome of FLAIR is also similar as T1, T2 and T1C.

COMPARATIVE LONGITUDINAL RELAXATION TIME ANALYSES

Among the variety of imaging modalities, Magnetic Resonance Imaging (MRI) shows most details of brain and is the most common test for diagnosis of brain tumors. MRI contains T1-weighted MRI (T1w), T1-weighted MRI with contrast enhancement (T1wc), T2-weighted MRI (T2w), Proton Density-Weighted MRI (PDw), Fluid-Attenuated Inversion Recovery (FLAIR), and so forth. Unlike Computed Tomography (CT) image, MRI images from different types of machines have different gray scale values.

This work also distinguishes the image representations for similar conditions for different patient and dissimilar condition for similar patient [Fig.1] [Fig.2] [Fig.3] [Fig.4] [Fig.5]. The sample is collected from BRATs 2015 dataset.

ISSN: 2277-9655
Impact Factor: 4.116
CODEN: IJESS7

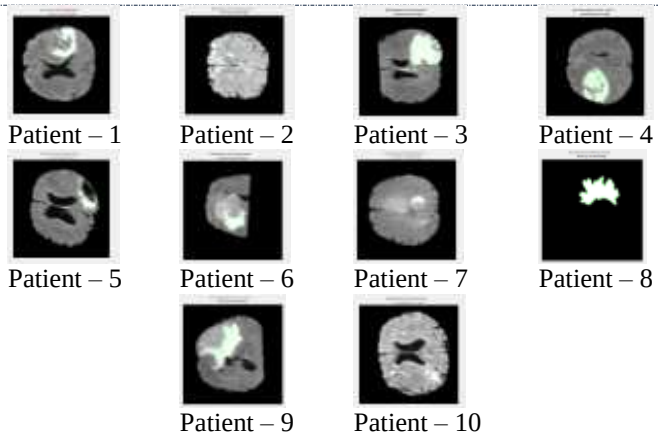

Fig. 1. FLAIR Image Format Analysis

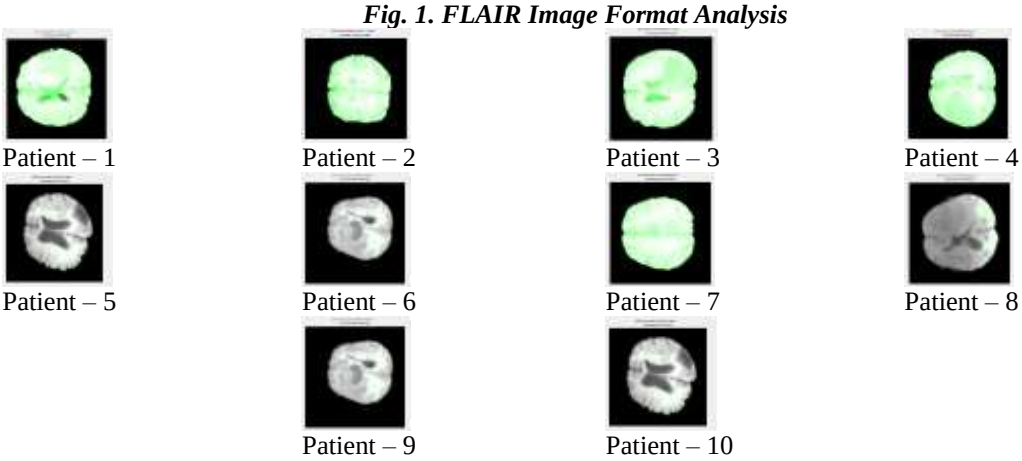

Fig. 2. T1 Image Format Analysis

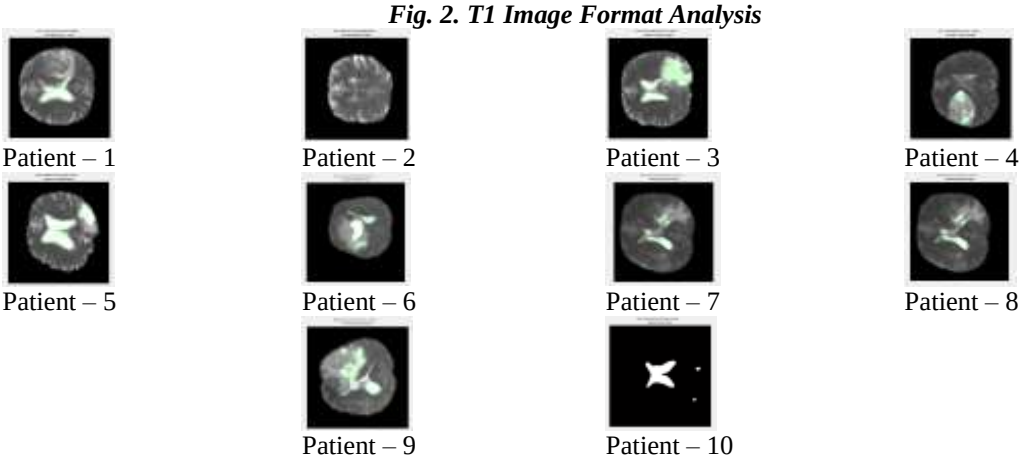

Fig. 3. T2 Image Format Analysis

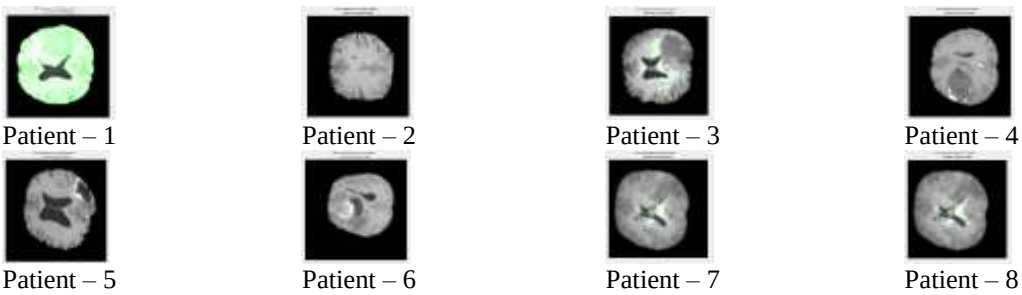

ISSN: 2277-9655
Impact Factor: 4.116
CODEN: IJESS7


Patient – 9


Patient – 10

Fig. 4. T1C Image Format Analysis


Patient – 1. Flair


Patient – 1. T1


Patient – 1. T2


Patient – 1. T1C


Patient – 2. Flair


Patient – 2. T1

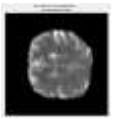
Patient – 2. T2

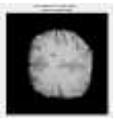
Patient – 2. T1C


Patient – 3. Flair


Patient – 3. T1

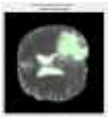
Patient – 3. T2


Patient – 3. T1C


Patient – 4. Flair


Patient – 4. T1

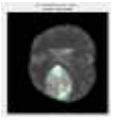
Patient – 4. T2

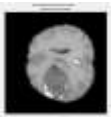
Patient – 4. T1C


Patient – 5. Flair


Patient – 5. T1


Patient – 5. T2


Patient – 5. T1C

Fig. 5. Visual Comparison of Same Patient in FLAIR, T1, T2 and T1C Image Format

PROPOSED FRAMEWORK

The major focus of this work is to increase the accuracy of the detection of brain anomalies for MR Images. The magnetic resonance techniques for generating the visual representation of brain images result in two different types of images as T1 image and T2 image. The studies demonstrate the accuracy of T1 images is higher for detecting the anomalies. Hence in this work we focus on T1 images to carry out the proposed method. The core framework is been demonstrated here [Fig. 6].

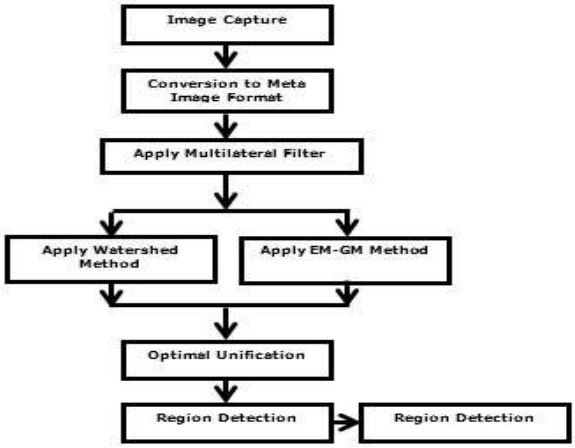

Fig. 6. Proposed framework for Brain Anomaly Detection

E. Novel Multilateral Filter

The Proposed multilateral filter is based on the existing bilateral filter for improving the input image variance and standard deviation [4] [11].

ISSN: 2277-9655
Impact Factor: 4.116
CODEN: IJESS7

The bilateral filter explained as

$$\overline{IMG}(Co_1) = \frac{1}{N(Co_1)} \sum_{Co_1 \in Px} IMG(Co_2).g(Co_1, Co_2).P(IMG(Co_2), IMG(Co_1)) \quad \text{(Eq. 5)}$$

Where,

IMG, denotes the original image

$\overline{IMG}$, denotes the filtered and noise removed image

Co_1 and Co_2, denotes the spatial coordinates of the image

Px, denotes the collection of pixels around the noise

$N(Co_1)$, denotes the normalization constant for each pixel to restrict the value after normalization within geometric and photonic range denoted by Px

And g and p, denotes the geometric and photometric similarities of the image

Hence the enhancement of the image is proposed to regularize the local signal amplitude of every pixel value:

$$\overline{IMG}(Co_1) = \frac{1}{N(Co_1)} \sum_{Co_1 \in Px} IMG(Co_2).\theta(Co_1, Co_2, t) \quad \text{(Eq. 6)}$$

As,

$$\theta(Co_1, Co_2, t) = (1 - a(Co_1)).g(Co_1, Co_2) + a(Co_1).g(Co_1, Co_2).P(IMG(Co_1), IMG(Co_2)).\sum_{i=1}^{D-1} d_i(Co_1, Co_2) \quad \text{(Eq. 7)}$$

Where,

$a(Co_1)$, denotes the regularized local signal amplitude of the pixel

di, denotes the image dimensions for during noise removal

F. Enhanced Watershed

The existing watershed method [3] [12] [13] is applied in this phase of the algorithm. Watershed method is generally used for morphological gradient-based segmentation. The outcome of this phase is segmented image for optimal unification with EM – GM method outputs.

G. Enhanced Expectation Maximization and Gaussian Mixture

The existing Gaussian mixture method [5] [6] [10] is applied for each pixel of the normalized image. After application of Gaussian mixture method, the expectation maximization needs to be applied. Thereafter, the Gaussian parameters are to be mapped into the score point and finally, the likelihood to be calculated to converge.

H. Novel Optimal Unification

The optimal unification of the result images are carried out in two phases. In the first phase, the images are been divided into segments and in the next phase from the input images the segments are been merged. The approach is demonstrated here:

Novel Segment Dividing Technique: Image1 and Image2 are the results from Watershed and EM-GM method respectively

Calculate the number of regions for Image1 and Image2 and store in n and m respectively

$$\Psi[IMG_1] \to n, \Psi[IMG_2] \to m \quad \text{(Eq. 8)}$$

Repeat Till n+m, where m=n denotes the size of the SegmentList arrays

$$\forall\{\Psi[IMG_1], \Psi[IMG_2]\} \quad \text{(Eq. 9)}$$

Compare All SegmentList1[n] and SegmentList2[m] to find the unique region

ISSN: 2277-9655
Impact Factor: 4.116
CODEN: IJESS7

$$\exists[\forall\{\Psi[IMG_1]\}]_{\forall!n_i \neq n_j}, \exists[\forall\{\Psi[IMG_2]\}]_{\forall!m_i \neq m_j} \quad \text{(Eq. 10)}$$

If SegmentList1[n] and SegmentList2[m] are unique, then Store the segmented regions into the SegmentList1, SegmentList2 from Image1 and Image2 respectively

$$\exists[\forall\{\Psi[IMG_1]\}]_{\forall!n_i \neq n_j} \rightarrow SegmentList_1$$

$$\exists[\forall\{\Psi[IMG_2]\}]_{\forall!m_i \neq m_j} \rightarrow SegmentList_2 \quad \text{(Eq. 11)}$$

STEP-1. Novel Segment Combining Technique: SegmentList1, SegmentList2 are obtained from the previous equalization
STEP-2. Calculate the number of regions for SegmentList1, SegmentList2 and store in n and m respectively
STEP-3. Repeat Till n+m, where m=n denotes the size of the SegmentList arrays
STEP-4. Compare each Segment from SegmentList1 and SegmentList2 to find the similar regions
STEP-5. If the regions are nearing neighbors, then combine the regions
STEP-6. Mark the regions with anomalies

Based on the region marks, this technique will predict the possible diseases [Table – 1] [9] [7] [8].

Table 1. Brain Anomalous Area and Prediction of Diseases

Brain Region	Predictable Diseases
Amygdala	Memory Loss, Anxiety, Phobia, Post – Traumatic Disorder
Prefrontal Cortex	Stress
Anterior Cingulate Cortex	ADHD, Schizophrenia, Depression
Hippocampus	Mood Disorder

The predictions of diseases are demonstrated in results and discussion section of this paper.

MULTILATERAL FILTER OUTCOMES

The improvement in the input images are been recorded [Table – 2 to 5] and the improvement in variance and standard deviation is been observed.

Table 2. Improvement in the Input Data by Multilateral Filter – FLAIR

Image Dataset In MHA	Actual Image Variance	Filtered Image Variance	Improvement	Actual Image Std. Deviation	Filtered Image Std. Deviation	Improvement
Patient – 1	5060902.713	4915045.117	0.02882	69.797568	69.568505	0.003282
Patient – 2	9554696.161	16036161.27	0.678354	77.144764	88.461004	0.146688
Patient – 3	8616966.903	9325425.899	0.082217	73.134012	74.266098	0.01548
Patient – 4	2898009.131	5441952.068	0.877824	58.438954	68.754658	0.176521
Patient – 5	3297844.713	3310126.799	0.003724	60.892958	61.294396	0.006593
Patient – 6	7956455.468	9209704.089	0.157513	61.032613	63.335792	0.037737
Patient – 7	4355136.222	4923593.077	0.130526	68.444576	70.463172	0.029492
Patient – 8	21368886.14	18066531.68	0.15454	63.106152	60.306925	0.044357
Patient – 9	7298752.498	8231411.34	0.127783	71.921236	73.941303	0.028087
Patient – 10	2239552.24	8164522.795	2.645605	60.061124	84.239216	0.402558

Table 3. Improvement in the Input Data by Multilateral Filter – T1

Image Dataset In MHA	Actual Image Variance	Filtered Image Variance	Improvement	Actual Image Std. Deviation	Filtered Image Std. Deviation	Improvement
Patient – 1	4426745.687	19162216.05	3.328737	72.648616	104.887534	0.443765
Patient – 2	8406091.46	26021378.86	2.095538	74.846144	99.801705	0.333425
Patient – 3	16958827.91	19501273.64	0.149919	100.156664	103.583045	0.03421
Patient – 4	17772628.04	19802241.38	0.114199	99.038213	102.016712	0.030074

ISSN: 2277-9655
Impact Factor: 4.116
CODEN: IJESS7

Patient – 5	13768559.75	14906214.22	0.082627	93.611389	95.94429	0.024921
Patient – 6	22898252.69	24819950.25	0.083923	93.447251	95.434675	0.021268
Patient – 7	22003154	24379743.81	0.108011	104.394753	106.962605	0.024598
Patient – 8	15379577.02	16119083.29	0.048084	103.211526	104.673618	0.014166
Patient – 9	9672979.152	11018602.43	0.139112	78.361981	81.946585	0.045744
Patient – 10	9672979.152	11018602.43	0.139112	78.361981	81.946585	0.045744

Table 4. Improvement in the Input Data by Multilateral Filter – T2

Image Dataset In MHA	Actual Image Variance	Filtered Image Variance	Improvement	Actual Image Std. Deviation	Filtered Image Std. Deviation	Improvement
Patient – 1	2893554.644	3752181.075	0.296738	60.258618	64.599329	0.072035
Patient – 2	2406414.584	3177258.438	0.320329	50.748587	56.46155	0.112574
Patient – 3	4859893.989	4779595.617	0.016523	66.462106	66.070983	0.005885
Patient – 4	1722850.314	2062650.347	0.197231	47.485555	49.923533	0.051341
Patient – 5	5053719.403	8311452.955	0.644621	63.456567	71.954974	0.133925
Patient – 6	5053719.403	8311452.955	0.644621	63.456567	71.954974	0.133925
Patient – 7	6116058.465	6181313.026	0.010669	56.694385	56.933726	0.004222
Patient – 8	1655927.918	1632738.103	0.014004	50.417798	50.442167	0.000483
Patient – 9	4688216.164	4697257.513	0.001929	68.233328	68.089125	0.002113
Patient – 10	3213676.027	3928247.099	0.222353	61.218723	65.484408	0.069679

Table 5. Improvement in the Input Data by Multilateral Filter – T1C

Image Dataset In MHA	Actual Image Variance	Filtered Image Variance	Improvement	Actual Image Std. Deviation	Filtered Image Std. Deviation	Improvement
Patient – 1	7293520.405	17192522.9	1.357232	80.733374	100.264884	0.241926
Patient – 2	1829464.97	10392524.45	4.680636	51.132055	79.382207	0.552494
Patient – 3	752554.5295	8586590.521	10.409925	43.737097	81.375867	0.860569
Patient – 4	1008211.942	6543428.922	5.490132	47.294959	76.133189	0.609753
Patient – 5	1823443.794	5016480.102	1.751102	54.81342	71.403739	0.302669
Patient – 6	3550669.136	9953151.433	1.803176	58.35015	75.674243	0.296899
Patient – 7	596971.6746	4443766.514	6.443848	45.598477	76.271296	0.672672
Patient – 8	596971.6746	4443766.514	6.443848	45.598477	76.271296	0.672672
Patient – 9	1948743.064	3492151.849	0.792002	52.0609	60.615936	0.164327
Patient – 10	1901077.531	7470530.45	2.92963	59.159467	84.129712	0.422084

The improvements are visualized in this section [Fig. 7 to 10].


Fig. 7. Improvement on T1 Format


Fig. 8. Improvement on FLAIR Format


Fig. 9. Improvement on T1C Format

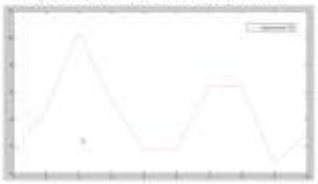
Fig. 10. Improvement on T2 Format

RESULTS AND DISCUSSION

The optimal unification framework is been applied to FLAIR, T1, T2 and T1C image formats alongside with the enhanced Watershed [Table – 6 to 9] and EM-GM [Table – 10 to 13] techniques and a relative improvement in the result is observed.

ISSN: 2277-9655
Impact Factor: 4.116
CODEN: IJESS7

Table 6. Accuracy Analysis over Watershed Method - FLAIR

Image Dataset In MHA format	Watershed	Novel Unification Technique	Improvement (%)
Patient – 1	98.01	99.01	1.02
Patient – 2	98.11	99.11	1.02
Patient – 3	97.66	98.66	1.02
Patient – 4	96.33	97.33	1.04
Patient – 5	96.35	97.35	1.04
Patient – 6	94.97	95.97	1.05
Patient – 7	92.65	93.65	1.08
Patient – 8	97.98	98.98	1.02
Patient – 9	90.92	91.92	1.10
Patient – 10	98.07	99.07	1.02

Table 7. Accuracy Analysis over Watershed Method - T1

Image Dataset In MHA format	Watershed	Novel Unification Technique	Improvement (%)
Patient – 1	98.13	99.13	1.02
Patient – 2	98.12	99.12	1.02
Patient – 3	97.99	98.99	1.02
Patient – 4	98	99	1.02
Patient – 5	95.36	96.36	1.05
Patient – 6	92.69	93.69	1.08
Patient – 7	97.98	98.98	1.02
Patient – 8	97.98	98.98	1.02
Patient – 9	85.43	86.43	1.17
Patient – 10	97	98	1.03

Table 8. Accuracy Analysis over Watershed Method - T2

Image Dataset In MHA format	Watershed	Novel Unification Technique	Improvement (%)
Patient – 1	96.06	97.03	1.01
Patient – 2	98.29	99.29	1.02
Patient – 3	96.05	97.05	1.04
Patient – 4	93.02	94.02	1.08
Patient – 5	95.6	96.6	1.05
Patient – 6	93.32	94.32	1.07
Patient – 7	92.42	93.42	1.08
Patient – 8	91.88	92.88	1.09
Patient – 9	88.47	89.47	1.13
Patient – 10	97.46	98.46	1.03

Table 9. Accuracy Analysis over Watershed Method - T1C

Image Dataset In MHA format	Watershed	Novel Unification Technique	Improvement (%)
Patient – 1	98.08	99.09	1.03
Patient – 2	98.29	99.29	1.02
Patient – 3	91.82	92.82	1.09
Patient – 4	91.97	92.97	1.09
Patient – 5	95.51	96.51	1.05
Patient – 6	93.3	94.3	1.07
Patient – 7	92.71	93.71	1.08
Patient – 8	91.62	92.62	1.09
Patient – 9	89.95	90.95	1.11

Patient – 10	97.62	98.62	1.02

The improvements are visualized here [Fig. 11 to 14]

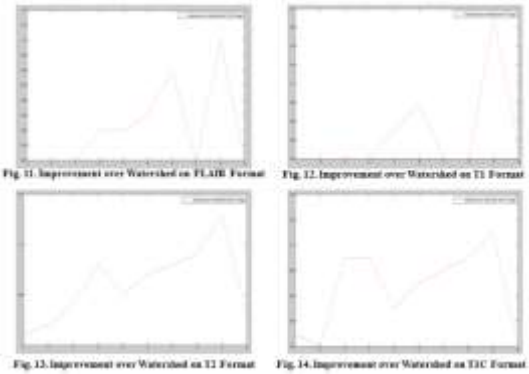

Table 10. Accuracy Analysis over Expectation Maximization – Gaussian Mixture Method – FLAIR

Image Dataset In MHA format	EM – GM	Novel Unification Technique	Improvement (%)
Patient – 1	97.78	99.01	1.26
Patient – 2	98.11	99.11	1.02
Patient – 3	97.02	98.02	1.03
Patient – 4	93.71	94.71	1.07
Patient – 5	95.87	96.87	1.04
Patient – 6	94.3	95.3	1.06
Patient – 7	92.48	93.48	1.08
Patient – 8	95.1	96.1	1.05
Patient – 9	89.28	90.28	1.12
Patient – 10	98.08	99.08	1.02

Table 11. Accuracy Analysis over Expectation Maximization – Gaussian Mixture Method – T1

Image Dataset In MHA format	EM – GM	Novel Unification Technique	Improvement (%)
Patient – 1	96.97	99.13	2.23
Patient – 2	98.12	99.12	1.02
Patient – 3	91.53	92.53	1.09
Patient – 4	91.67	92.67	1.09
Patient – 5	95.63	96.63	1.05
Patient – 6	93.04	94.04	1.07
Patient – 7	94.25	95.25	1.06
Patient – 8	92.03	93.03	1.09
Patient – 9	85.43	86.43	1.17
Patient – 10	97.54	98.54	1.03

Table 12. Accuracy Analysis over Expectation Maximization – Gaussian Mixture Method – T2

Image Dataset In MHA format	EM – GM	Novel Unification Technique	Improvement (%)
Patient – 1	95.99	97.03	1.08
Patient – 2	98.29	99.29	1.02
Patient – 3	91.64	92.64	1.09
Patient – 4	91.86	92.86	1.09
Patient – 5	95.36	96.36	1.05
Patient – 6	92.87	93.87	1.08
Patient – 7	92.18	93.18	1.08
Patient – 8	91.57	92.57	1.09
Patient – 9	85.5	86.5	1.17

ISSN: 2277-9655
Impact Factor: 4.116
CODEN: IJESS7

Patient – 10	97.46	98.46	1.03

Table 13. Accuracy Analysis over Expectation Maximization – Gaussian Mixture Method – T1C

Image Dataset In MHA format	**EM – GM**	**Novel Unification Technique**	**Improvement (%)**
Patient – 1	95.86	99.09	3.37
Patient – 2	98.29	99.29	1.02
Patient – 3	91.75	92.75	1.09
Patient – 4	91.99	92.99	1.09
Patient – 5	95.61	96.61	1.05
Patient – 6	93.27	94.27	1.07
Patient – 7	93.15	94.15	1.07
Patient – 8	91.62	92.62	1.09
Patient – 9	85.85	86.85	1.16
Patient – 10	97.86	98.86	1.02

The improvements are visualized here [Fig. 15 to 18]

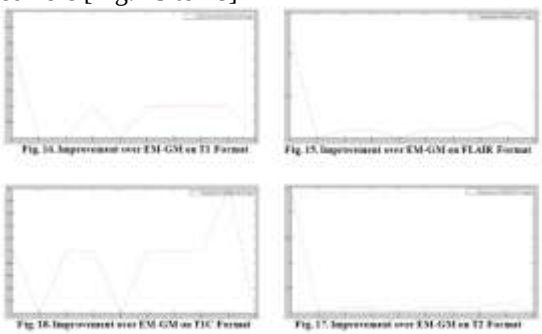

Hence this work shows the improvement of accuracy for all the tested datasets for 10 patients' dataset. The work also successfully predicts the diseases based on the anomalies detected on the brain regions. The outcomes of the predictive analysis is also demonstrated [Fig. 21] [Table – 14].

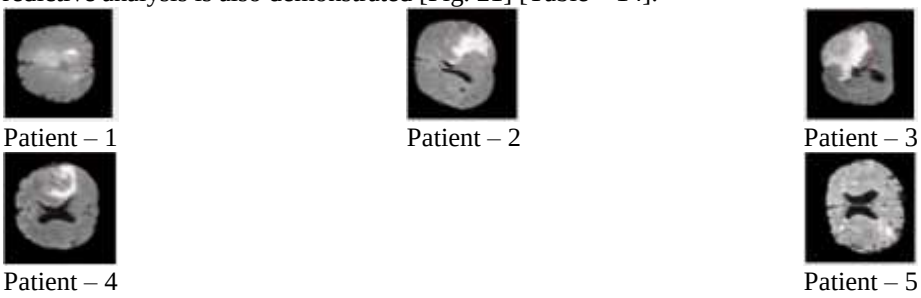

Fig. 19. Disease Prediction for Various Patients

Table 14. Region Based Disease Prediction Results

Image Dataset In MHA format	**Regions Detected**	**Predicted Diseases**
Patient – 1	Hippocampus – Right	Mood Disorder
Patient – 2	Anterior Cingulate Cortex	ADHD, Schizophrenia, Depression
Patient – 3	Prefrontal Cortex and Amygdala	Stress, Memory Loss, Anxiety, Phobia, Post – Traumatic Disorder

ISSN: 2277-9655
Impact Factor: 4.116
CODEN: IJESS7

Patient – 4	Anterior Cingulate Cortex	ADHD, Schizophrenia, Depression
Patient – 5	Hippocampus – Left	Mood Disorder

This outcome makes the work unique in nature and reduced the span of further investigations.

CONCLUSIONS

Major Contributions of this work are the multilateral filter to normalize the image noises and the enhancement of watershed and EM-GM technique to improve the detection of brain diseases. Quantitative analysis of brain MR images allows a greater understanding of the nature of the diseases. The proposed algorithm in this work has been tested on BRATS 2012 (Nice), BRATS 2013 (Nagoya) and BRATS 2014 (Boston) challenge datasets and demonstrates higher accuracy. The work also concludes the optimal technique for medical image segmentation and detection of brain anomalies. Compared to the existing research outcomes, this work demonstrates the mapping of possible disease with the brain anomalous regions. With the final outcome of accuracy improvement for FLAIR, T1, T2 and T1C image data types on disease prediction, the work certainly and satisfyingly extends the possibilities of better medical image processing.

REFERENCES

[1] N. Porz, "Multi-modalodal glioblastoma segmentation: Man versus machine", PLOS ONE, vol. 9, pp. e96873, 2014
[2] S. Bauer, R. Wiest, L.-P. Nolte and M. Reyes, "A survey of MRI-based medical image analysis for brain tumor studies", Phys. Med. Biol., vol. 58, no. 13, pp. R97-R129, 2013
[3] D. W. Shattuck, G. Prasad, M. Mirza, K. L. Narr and A. W. Toga, "Online resource for validation of brain segmentation methods", Neuroimage, vol. 45, no. 2, pp. 431-439, 2009
[4] M. Stille, M. Kleine ; J. Hagele ; J. Barkhausen ; T. M. Buzug, "Augmented Likelihood Image Reconstruction", IEEE Transactions on Medical Imaging, Volume:35, Issue:1
[5] A. Gooya, G. Biros and C. Davatzikos, "Deformable registration of glioma images using EM algorithm and diffusion reaction modeling", IEEE Trans. Med. Imag., vol. 30, no. 2, pp. 375-390, 2011
[6] L. Weizman, "Automatic segmentation, internal classification, and follow-up of optic pathway gliomas in MRI", Med. Image Anal., vol. 16, no. 1, pp. 177-188, 2012
[7] K. Hameeteman, "Evaluation framework for carotid bifurcation lumen segmentation and stenosis grading", Med. Image Anal., vol. 15, no. 4, pp. 477-488, 2011
[8] S. Ahmed, K. M. Iftekharuddin and A. Vossough, "Efficacy of texture, shape, and intensity feature fusion for posterior-fossa tumor segmentation in MRI", IEEE Trans. Inf. Technol. Biomed., vol. 15, no. 2, pp. 206-213, 2015
[9] R. Achanta et al., "SLIC superpixels compared to state-of-the-art su- perpixel methods," IEEE Trans. Pattern Anal. Mach. Intell., vol. 34, no. 11, pp. 2274–2282, Nov. 2012
[10] B. B. Avants et al., "A reproducible evaluation of ANTs similarity metric performance in brain image registration," Neuroimage, vol. 54, no. 3, pp. 2033–44, Feb. 2011
[11] N. Subbanna, D. Precup, L. Collins, and T. Arbel, "Hierarchical prob- abilistic Gabor and MRF segmentation of brain tumours in MRI vol- umes," Proc. MICCAI, vol. 8149, pp. 751–758, 2013
[12] H. C. Shin, M. R. Orton, D. J. Collins, S. J. Doran, and M. O. Leach, "Stacked autoencoders for unsupervised feature learning and multiple organ detection in a pilot study using 4D patient data," IEEE Trans. Pattern Anal. Mach. Intell., vol. 35, no. 8, pp. 1930–1943, Aug. 2013
[13] A. Islam, S. M. S. Reza, and K. M. Iftekharuddin, "Multi-fractal texture estimation for detection and segmentation of brain tumors," IEEE Trans. Biomed. Eng., vol. 60, no. 11, pp. 3204–3215, Nov. 2013.

CITE AN ARTICLE:

P, N. R., Rao, C. M., & Satyanarayana, C. (2017). RELIABILITY ANALYSIS OF ANOMALIES AND DISEASE PREDICTION USING NOVEL OPTIMAL SEGMENTATION FRAMEWORK FOR VARIOUS NON – EQUILIBRIUM BRAIN TISSUE ANGULAR MOMENTUM. *INTERNATIONAL JOURNAL OF ENGINEERING SCIENCES & RESEARCH TECHNOLOGY, 6*(5), 154-271. doi:10.5281/zenodo.573547